Overexpressing IRS1 in Endothelial Cells Enhances Angioblast Differentiation and Wound Healing in Diabetes and Insulin Resistance

Sayaka Katagiri,[1] Kyoungmin Park,[1] Yasutaka Maeda,[1] Tata Nageswara Rao,[2] Mogher Khamaisi,[1] Qian Li,[1] Hisashi Yokomizo,[1] Akira Mima,[1] Luca Lancerotto,[3] Amy Wagers,[2] Dennis P. Orgill,[3] and George L. King[1]

Overexpressing IRS1 in Endothelial Cells Enhances Angioblast Differentiation and Wound Healing in Diabetes and Insulin Resistance

Diabetes 2016;65:2760–2771 | DOI: 10.2337/db15-1721

The effect of enhancing insulin's actions in endothelial cells (ECs) to improve angiogenesis and wound healing was studied in obesity and diabetes. Insulin receptor substrate 1 (IRS1) was overexpressed in ECs using the VE-cadherin promoter to create ECIRS1 TG mice, which elevated pAkt activation and expressions of vascular endothelial growth factor (VEGF), Flk1, and VE-cadherin in ECs and granulation tissues (GTs) of full-thickness wounds. Open wound and epithelialization rates and angiogenesis significantly improved in normal mice and high fat (HF) diet–induced diabetic mice with hyperinsulinemia in ECIRS1 TG versus wild type (WT), but not in insulin-deficient diabetic mice. Increased angioblasts and EC numbers in GT of ECIRS1 mice were due to proliferation in situ rather than uptake. GT in HF-fed diabetic mice exhibited parallel decreases in insulin and VEGF-induced pAkt and EC numbers by >50% without changes in angioblasts versus WT mice, which were improved in ECIRS1 TG mice on normal chow or HF diet. Thus, HF-induced diabetes impaired angiogenesis by inhibiting insulin signaling in GT to decrease the differentiation of angioblasts to EC, which was normalized by enhancing insulin's action targeted to EC, a potential target to improve wound healing in diabetes and obesity.

Every step of the complex process of wound healing has been reported to be defective, including impairments of neutrophil activation and responses, fibroblast migration and proliferation, and angiogenesis (1–5). Poor glycemic control, neuropathy, presence of micro- and macrovascular complications, and insulin resistance are associated with impaired wound healing (6). Most strategies devised to improve chronic wound healing in patients with diabetes have not exhibited clear efficacy, possibly due to a lack of full understanding of the mechanisms induced by diabetes to impair the wound healing process (5–8).

One major factor that contributes to impaired wound healing in diabetic and insulin-resistant states is reduced angiogenesis in the granulation tissue (GT), which could be the result of decreased vascular endothelial growth factor (VEGF) expression or its actions in response to hypoxia (4,9,10). Multiple metabolic abnormalities can affect VEGF expression and actions, including hyperglycemia-related oxidative stress, glycation products, and activation of protein kinase C (PKC) (10–13). Systemic insulin resistance could also affect angiogenesis because insulin's signaling can regulate VEGF expression, which has been reported to be inhibited in diabetes (14,15). Thus, we postulate that insulin resistance may exist in the GT to impair angiogenesis, by inhibiting insulin signaling to enhance VEGF expression and actions.

Insulin receptors are present in many cells of the GT, including keratinocytes, fibroblasts, endothelial cells (ECs), and inflammatory cells (16–21). Mice with deletion of insulin receptors in the fibroblasts and myocardium exhibited decreases in VEGF expression and capillary density in response to hypoxia (14). Insulin can induce VEGF expression mostly through the IRS1/PI3K/Akt pathway, which is selectively inhibited in insulin resistance and diabetes (14,15,22–24). Activation of pAkt affected VEGF

[1]Section of Vascular Cell Biology, Joslin Diabetes Center, Harvard Medical School, Boston, MA
[2]Department of Stem Cell and Regenerative Biology, Harvard Stem Cell Institute, Joslin Diabetes Center, Havard Medical School, Boston, MA
[3]Division of Plastic Surgery, Brigham and Women's Hospital, Harvard Medical School, Boston, MA
Corresponding author: George L. King, george.king@joslin.harvard.edu.

Received 17 December 2015 and accepted 15 May 2016.
This article contains Supplementary Data online at http://diabetes.diabetesjournals.org/lookup/suppl/doi:10.2337/db15-1721/-/DC1.

secretion in keratinocytes and angiogenesis in cutaneous wound healing (25–27). The finding that insulin resistance may impair wound healing also suggests that differential pathogenic mechanisms may exist for defective wound healing associated with diabetes due to insulin deficiency or resistance with hyperinsulinemia. This study investigated the regulation of the insulin signaling pathway in GT and on the differentiation of angioblasts to ECs in the GT using rodent diabetic models of insulin deficiency or hyperinsulinemia and insulin resistance.

RESEARCH DESIGN AND METHODS

Wild-type (WT) C57/BL6J mice were purchased from The Jackson Laboratory (Bar Harbor, ME). Recombinant human VEGF (R&D Systems, Minneapolis, MN) and antibodies to pAkt, Akt, pErk, Erk1/2, fibronectin, IRS1 (Cell Signaling, Danvers, MA), VCAM1 (Millipore, Billerica, MA), Flk1, eNOS (BD Biosciences, San Jose, CA), and β-actin (Santa Cruz Biotechnology Inc., Santa Cruz, CA) were obtained commercially.

Animals

All protocols for animal use and euthanasia were approved by the Animal Care Committee of the Joslin Diabetes Center and are in accordance with National Institutes of Health (NIH) guidelines. Mice with endothelial-specific overexpression of IRS1 (ECIRS1 TG) with VE-cadherin promoter were described previously (28) (Supplementary Fig. 1*A*). The following primers were used for IRS1 genotyping: 5′-ATCTGCAGGCAGCTCACAAAG-3′ and 5′-CGAA GAAGCGTTTGTGCATGC-3′. Two mice models of diabetes were used. *1*) For hyperinsulinemia with insulin resistance and hyperglycemia, male mice at age 4 weeks were fed with normal chow (NC) (3.3% kcal fat) or high fat (HF) (60% kcal fat) for 10 weeks (28). Insulin-deficient diabetic mice were produced by five consecutive days of intraperitoneal injection of 50 mg streptozotocin (STZ)/kg body weight (Sigma-Aldrich, St. Louis, MO), and fasting blood glucose concentrations >400 mg/dL were documented. Insulin treatment was performed using insulin pellet (LinShin Canada, Inc., Scarborough, Ontario, Canada) placed subcutaneously and with a release rate of 0.1 unit/day/insulin pellet, which was adjusted to maintain plasma glucose at 150 mg/dL range (at steady state) in STZ-induced diabetic mice for 2 weeks. Intraperitoneal glucose tolerance tests (IPGTTs) were performed as previously described (29).

Wound Healing Model

Mouse dorsal hair was depilated on the day before surgery (Nair; Church & Dwight Co., Inc., Ewing, NJ), and mice were anesthetized by isoflurane inhalation (isoflurane, USP; NOVAPLUS, Lake Forest, IL). Their dorsum was disinfected with 70% alcohol and marked with standard square template (1.0 cm^2). Skin plus panniculus carnosus was excised to create a full-thickness dorsal excisional wound, which was covered with transparent, semiocclusive adhesive polyurethane dressings (Tegaderm; 3M, St. Paul, MN) and changed two times per week (30–32).

Tissue Morphometric Analysis

Digital macroscopic images of the wound were analyzed using NIH ImageJ software version 1.40 (Bethesda, MD). Standardized photographs were taken on the day of surgery and on the 3rd, 7th, 10th, and 14th days for 14 days from a standard height. Re-epithelialization and open wound surface were measured as a percentage of the initial wound area as published (30–32).

Wound kinetics were quantified as follows: open wound rate (OWR) = open wound/initial area of wound size, contraction rate (CR) = contraction/initial area of wound size, and epithelialization rate (ER) = epithelialization/initial area of wound size − contraction (30,31). On days 3, 7, and 10 postsurgery, wounds from seven to eight animals in each group were harvested as previously described (32).

For signaling studies, insulin (1 unit/kg body weight) was administrated intravenously and GTs were collected 10 min afterward. For histological studies, excised tissues were fixed in 4% formalin at 4°C. Panoramic cross-sectional digital images of each wound were examined using an FSX100 microscope (Olympus, Center Valley, CA).

Immunofluorescence Studies

Immunohistochemistry studies were performed using paraffin sections and incubated with 0.5% BSA and rabbit mAbs to CD31 (Dianova GmbH, Hamburg, CA) as primary antibody to identify EC, followed by Alexa Flour 488–conjugated secondary antibodies (Invitrogen, Gland Island, NY). Nuclei were counterstained with DAPI (Invitrogen). Quantitative fluorescent analyses were performed using an FSX100 microscope and Adobe Photoshop *CS* Software (San Jose, CA).

Immunoblot and Immunoprecipitation Studies

GT, frozen in dry ice, was homogenized in ice-cold tissue lysis buffer, as previously described (33). Protein concentration was determined by Bradford assay and processed as previously described (33).

Real-Time PCR

Real-time PCR procedures were used to assess mRNA levels (Applied Biosystems, Grand Island, NY) and normalized to 36B4 or 18*S* rRNA. PCR primers used in the study are listed in Supplementary Table 1.

Culture of ECs

Lung tissues from c57/BL6J mice were used to obtain primary ECs and used between passages three and five (33,34). ECs were incubated for 16 h in DMEM containing 0.1% BSA and stimulated with 100 nmol/L insulin for 24 h. Expression of VEGF165 in media was measured by an ELISA kit (R&D Systems).

Bone Marrow Cell Transplantation

Bone marrow (BM) cells from green fluorescent protein (GFP)–expressing mice (The Jackson Laboratory) were harvested from tibias and femurs by flushing with Dulbecco's PBS + 5% FBS and were resuspended and filtered through a

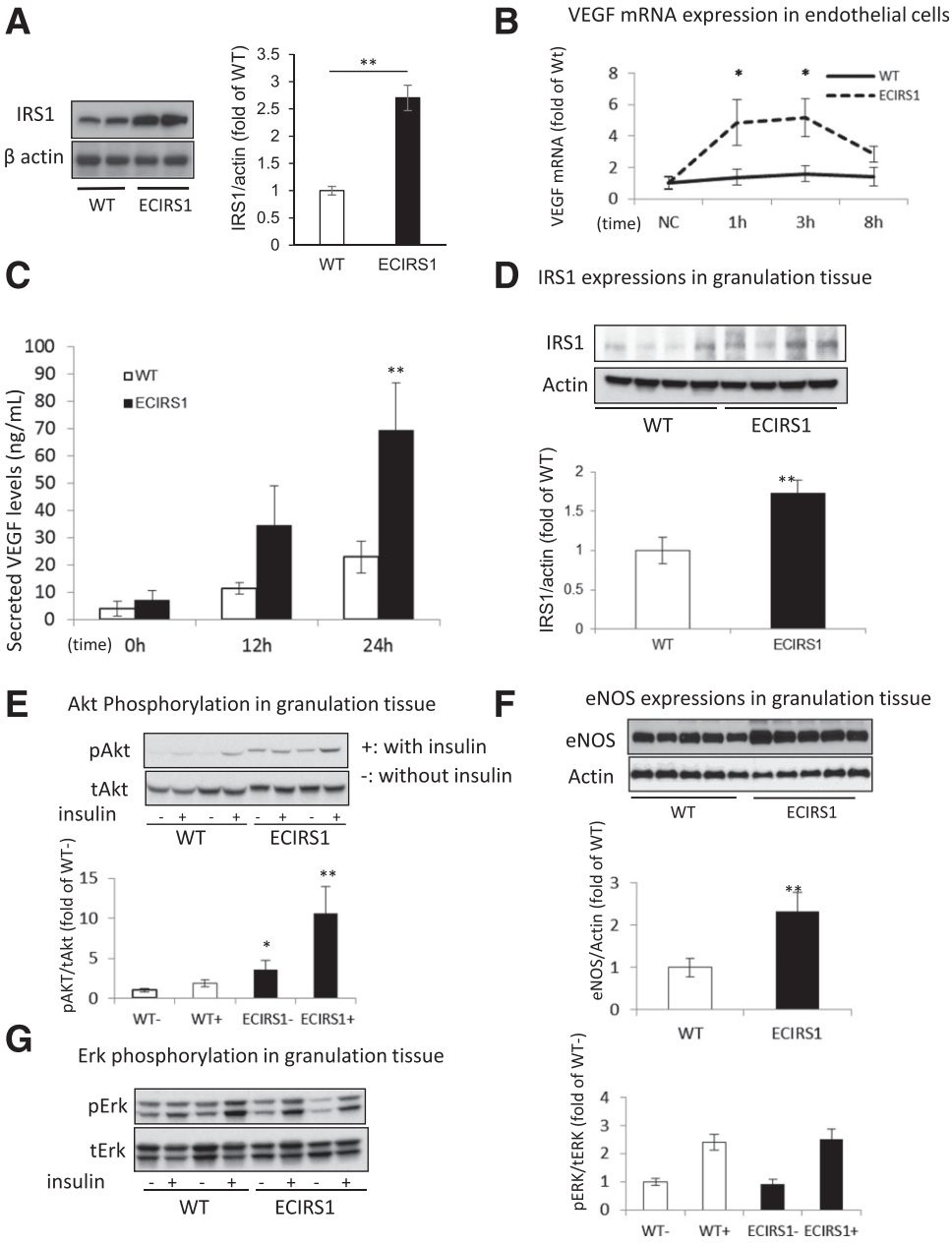

Figure 1—Characterization of insulin signaling and VEGF expression in lung ECs and GT of WT and ECIRS1 TG mice. *A*: IRS1 protein expression in lung ECs. *B*: VEGF mRNA expressions in cultured ECs from WT and ECIRS1 TG mice with insulin stimulation (100 nmol/L) at 1, 3, and 8 h. *C*: Secreted VEGF protein levels in the media of cultured ECs from WT and ECIRS1 TG mice with insulin stimulation (100 nmol/L) at 0, 12, and 24 h. *D*: IRS1 protein expressions in GT in WT and ECIRS1 TG mice at 7 days postsurgery. *E*: Total Akt (tAkt) and pAkt expressions at 7 days in GT. *F*: eNOS expression in GT. *G*: Total Erk (tErk) and pErk expressions in GT. $^{*}P < 0.05$; $^{**}P < 0.01$. $n = 4$ in *A* and $n = 5$ in *B*–*G*.

70-μm cell strainer (35). Erythrocytes were depleted using ACK lysis buffer (Lonza, Basel, Switzerland). BM cells were stained with lineage marker mix (Lin: anti-CD3e [17-A2], anti-CD4 [L3T4], anti-CD8 [53-6.72], anti-B220 [RA3-6B2], anti–TER-119, anti–Gr-1 [RB6-8C5], and anti–Mac-1 [M1/70]; eBioscience, San Diego, CA). Flow cytometry–sorted lineage-negative cells were transplanted intravenously (2×10^6 cells/mouse) into congenic recipient mice and analyzed 7 days after transplantation (36).

Evaluating Proliferation In Vivo

At 4 and 6 days postwounding, BrdU (100 μL) was injected intraperitoneally and BrdU in angioblasts or ECs from blood and GT was detected by flow cytometry after 7 days (FITC BrdU Flow Kits; BD Pharmingen, San Jose, CA) (37).

Flow Cytometry of Cells in GT

Dissected GTs were incubated with collagenase I and II, DNase, and hyaluronidase in Hepes buffer for 30 min at 37°C

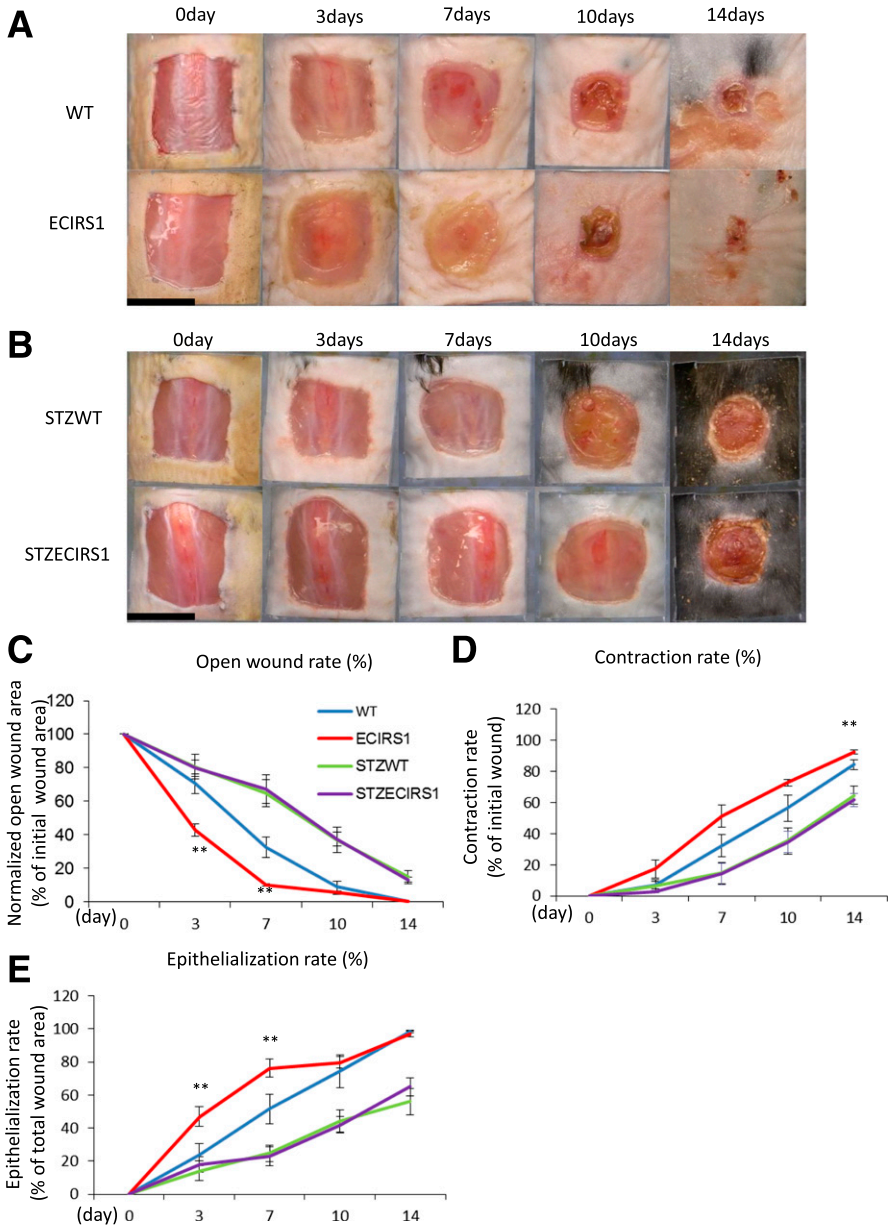

Figure 2—Comparison of wound healing among WT, ECIRS1 TG, STZWT, and STZECIRS1 TG mice. *A*: Photographs of wound at 0, 3, 7, 10, and 14 days in WT and ECIRS1 TG mice. *B*: STZWT and STZECIRS1 mice. Black bars, 1 cm. *C*: OWR. *D*: CR. *E*: ER ($n = 5$). $^{**}P < 0.01$.

and then filtered through a 70-μm cell strainer with erythrocytes depleted by ACK lysis buffer. Cells were incubated with insulin (100 nmol/L) and anti-CD16/32 (BioLegend, San Diego, CA), fixed in 2% formaldehyde, and permeabilized using the Perm/Wash Buffer (BD Biosciences, San Diego, CA) followed by incubation with monoclonal antibodies: anti-CD45 for leukocyte, anti-CD31 for EC, or anti-Flk1, marker for angioblast and PI for viability. Rabbit anti-Akt and rabbit anti–phospho-Akt (Ser473) were used to detect Akt activation, which were followed with Alexa Fluor 647 goat anti-rabbit IgG. All populations were routinely k-gated to verify purity and gating. One million cells from BM or 200,000 cells from GT were analyzed using FlowJo software version 10.0 (Tree Star, Inc., Ashland, OR).

Statistical Analysis

Values are expressed as mean and SEM. Student *t* tests were performed for comparison of two groups. One-way ANOVA, followed with Tukey-Kramer, was performed for comparisons of multiple groups using SPSS 22.0 (SPSS, Inc., Chicago, IL). A value of $P < 0.05$ was considered significant.

RESULTS

Characterization of ECIRS1 Transgenic Mice and Insulin Signaling in GT

To enhance insulin's actions, IRS1 was overexpressed in the EC using VE-cadherin promoter to produce ECIRS1 TG mice, which elevated IRS1 expression in the EC by

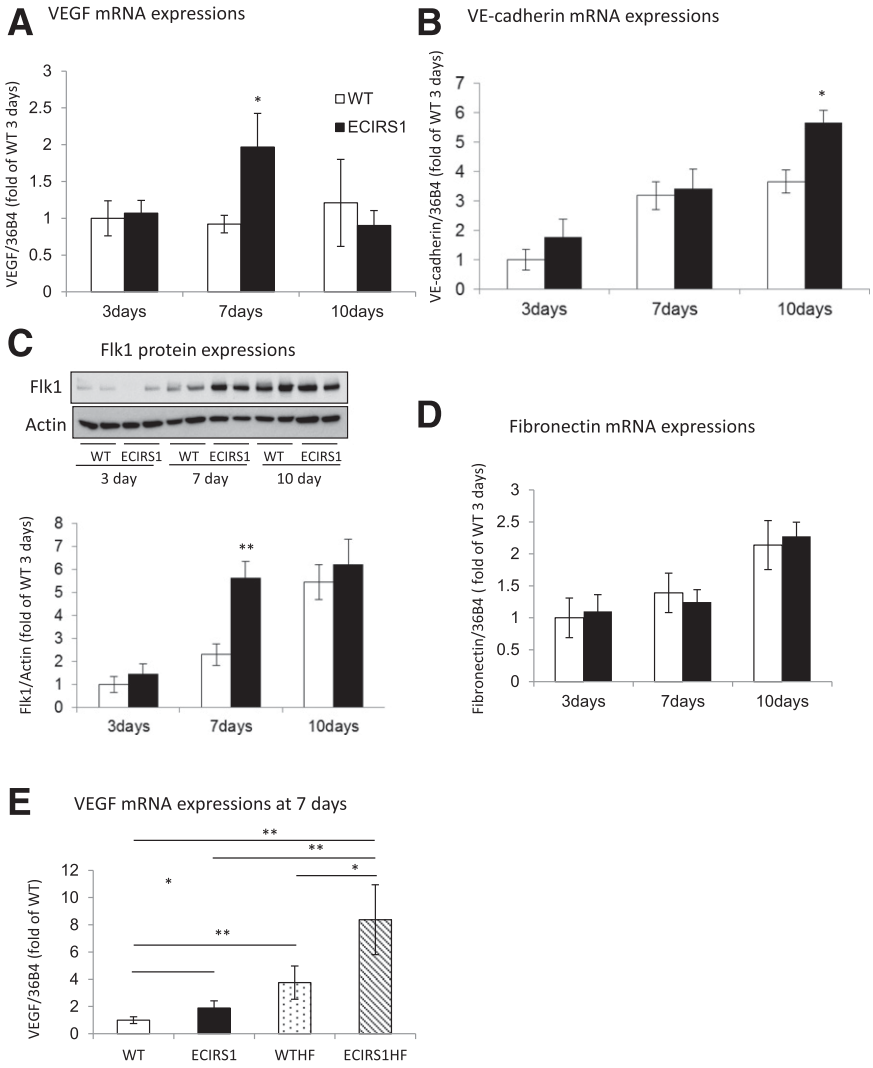

Figure 3—Analysis of genes for vessels in GT in VEGF mRNA expressions (*A*), VE-cadherin mRNA expressions (*B*), Flk1 expression (*C*), and fibronectin mRNA (*D*) at 3, 7, and 10 days postsurgery in the GT from WT and ECIRS1 TG mice ($n = 7$ at each time point). *E*: VEGF mRNA levels in the GTs from WT, ECIRS1, WTHF, and ECIRS1HF mice at 7 days postsurgery. *$P < 0.05$; **$P < 0.01$. $n = 7$.

170% and in the lung and retina, but not in peripheral blood mononuclear cells (Fig. 1*A* and Supplementary Fig. 1*B* and *C*). Metabolically, WT and ECIRS1 TG mice did not differ by glucose tolerance as measured by IPGTT and fasting plasma insulin levels (Supplementary Fig. 1*D* and *E*).

Insulin increased VEGFB mRNA expression by 240% at 1 and 3 h and protein levels in the media by 200% after 24 h in ECs from ECIRS1 TG mice versus WT mice (Fig. 1*B* and *C*). IRS1 protein expression was increased in GT from ECIRS1 TG mice by 72% as compared with WT mice ($P < 0.01$) (Fig. 1*D*). Further, Akt phosphorylation (pAkt) in the GT of ECIRS1 TG mice was significantly increased at basal (261%, $P < 0.05$) and after the addition of insulin (480%, $P < 0.01$) compared with WT (Fig. 1*E*), without a difference in insulin's activation of Erk (pErk) (Fig. 1*G*). Expressions of eNOS, a marker of capillary density, in the GT also significantly increased by 133%, comparing ECIRS1 TG to WT mice. (Fig. 1*F*).

Insulin's Actions on Wound Healing in Control and STZ-Induced Diabetic Mice

The effect of increasing IRS1 expression and insulin's actions in EC on wound healing was evaluated by comparing OWR, CR, and ER in WT and ECRIS1 TG mice (Fig. 2*A* and *B*). The results indicated that OWR decreased more rapidly in ECRS1 TG mice versus WT mice with improvements at 3 and 7 days ($P < 0.01$) (Fig. 2*C*). CR was significantly improved on day 14 and ER was increased in ECRIS1 TG mice by 96 and 48% on 3 and 7 days, respectively (Fig. 2*D* and *E*). VEGF mRNA and FLK1 protein expressions in the GT were also increased significantly on day 7, and VE-cadherin expression was increased on day 10 (Fig. 3*E*). No changes in fibronectin were observed comparing ECIRS1 TG to WT mice (Fig. 3*C*).

STZ-induced diabetic ECIRS1 TG and WT mice had comparable weights and fasting blood glucose of >500 mg/dL during the study (Supplementary Fig. 2*A* and *B*),

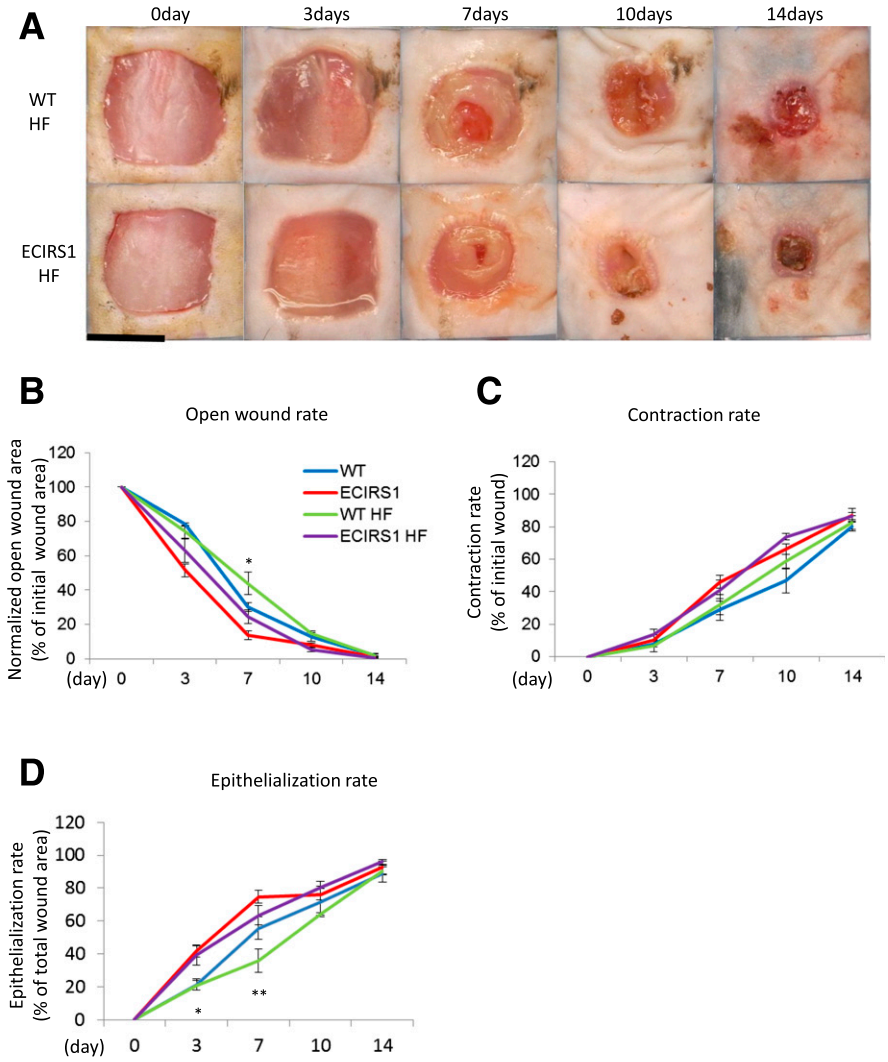

Figure 4—Comparison of wound healing among WT, ECIRS1, WTHF, and ECIRS1HF mice. *A*: Photographs of wound at 0, 3, 7, 10, and 14 days after surgery. Black bar, 1 cm. *B*: OWR (%). *C*: CR (%). *D*: ER (%) (n = 5 for each type of mice and at each time point). *P < 0.05; **P < 0.01.

with comparable plasma insulin levels of <0.2 ng/mL, which were four times lower than nondiabetic mice (Supplementary Fig. 2*C*). STZ diabetes delayed OWR, CR, and ER significantly, compared with nondiabetic WT and ECIRS1 TG mice at 3 and 7 days (Fig. 2*A*–*E*), although no differences were observed between diabetic STZWT and STZECIRS1 TG mice. VEGF mRNA expression in the GT after 7 days of wound initiation was decreased by 38% in STZ WT versus WT mice ($P < 0.05$) and in STZECIRS1 versus ECIRS1 mice ($P < 0.01$) (Supplementary Fig. 2*D*). We also evaluated wound healing between STZWT mice treated with insulin (STZWTins) and STZECIRS1 mice treated with insulin (STZECIRS1ins). The results showed that OWR was decreased ($P < 0.05$) and ER was increased ($P < 0.01$) in STZECIRS1ins mice compared with STZWTins mice at 7 days after injecting (Supplementary Fig. 3*A*–*D*).

Assessment of HF Diet–Induced Diabetes and Hyperinsulinemia on Wound Healing

To determine whether diabetes and hyperinsulinemia affect wound healing, we studied HF feeding in ECIRS1 TG (ECIRS1HF) and WT (WTHF) mice. After 10 weeks of HF feeding, body weights were significantly increased in both WTHF and ECIRS1HF mice compared with NC. Fasting blood glucose levels were elevated equally in both WTHF and ECIRS1HF mice to >200 mg/dL (Supplementary Fig. 4*A* and *B*). IPGTTs were similarly elevated; fasting and postinfusion glucose levels at 15 min >500 mg/dL (Supplementary Fig. 4*C*). Fasting plasma insulin levels increased significantly from 0.5 to 2.5 and 3.2 ng/dL in WTHF and ECIRS1HF mice (Supplementary Fig. 4*D*). Fasting plasma IGF1 level also increased in ECIRS1HF and WTHF mice (Supplementary Fig. 4*E*). Interestingly, VEGF mRNA expressions were increased in WTHF versus WT mice ($P < 0.05$) and in

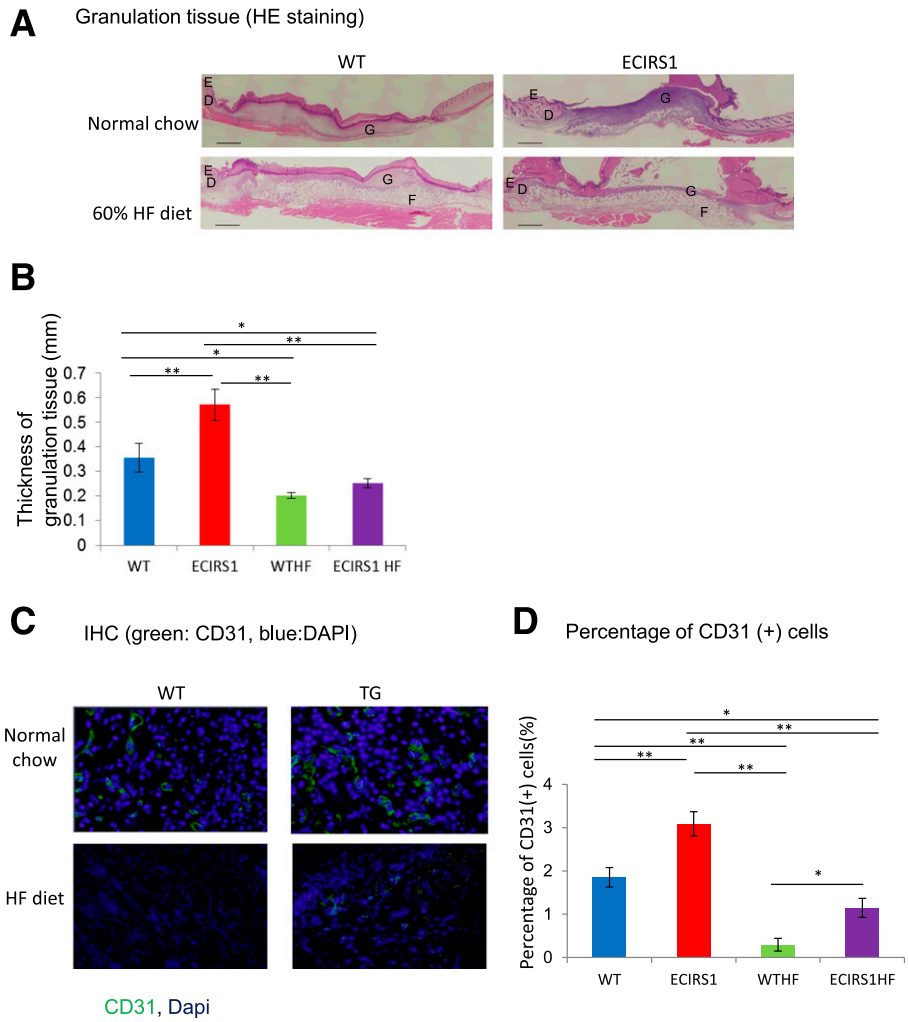

Figure 5—Histological analysis of the wound 7 days postsurgery in WT, ECIRS1, WTHF, and ECIRS1HF mice. *A*: Hematoxylin-eosin (HE)–stained photograph. Black bar, 1 cm. *B*: Thickness of GT (n = 5). *C*: Immunohistochemistry (IHC) of GT. Blue, DAPI; green, CD31. *D*: Percentage of CD31$^+$ cells isolated from GT (n = 5). *P < 0.05; **P < 0.01. D, dermis; E, epidermis; F, fatty tissue; G, GT.

ECIRS1HF versus ECIRS1 TG mice by 276 and to 341%, respectively (Fig. 3*E*). Analysis of the wound showed HF feeding delayed OWR and ER at 3 and 7 days. Further, ECIRS1HF mice had a significantly greater reduction in OWR and increased ER than WTHF mice at 3 and 7 days (Fig. 4*A*, *B*, and *D*). Thickness of GT measured at 7 days after surgery was greater in ECIRS1 TG versus WT mice ($P < 0.01$). HF feeding decreased GT thickness in both WTHF and ECIRS1HF mice ($P < 0.05$) (Fig. 5*A* and *B*). Immunohistological analysis of the GT showed the number of CD31$^+$ cells, a marker for ECs and capillaries, was increased in ECIRS1 TG versus WT mice ($P < 0.01$). HF feeding for 10 weeks decreased CD31$^+$ cells by 84% in WTHF versus WT mice (Fig. 5*C* and *D*) and decreased by 63% in ECIRS1HF versus ECIRS1 TG mice. However, a 290% elevation of CD31$^+$ cell numbers was observed in ECIRS1HF versus WTHF mice ($P < 0.05$) (Fig. 5*C* and *D*).

Assessing HF Diet–Induced Insulin Resistance and Diabetes on Angioblast and EC Distributions in GT

To characterize the potential mechanism for the reduction of ECs in the GT associated with HF diet, the distribution of angioblasts and ECs in the GT of WT and ECIRS1 TG mice on NC and HF were characterized. Angioblasts were identified by FLK1$^+$, PI$^-$, CD45$^-$, and CD31$^-$, and ECs by CD45$^-$, PI$^-$, and CD31$^+$ cell staining. Angioblast numbers increased significantly by 50% in ECIRS1 TG compared with WT mice and by 65% in ECIRS1HF versus WTHF mice (Fig. 6*A* and *B*). Interestingly, the elevations of angioblast levels were similar between NC- and HF-fed WT and ECIRS1 TG mice. EC numbers in GT increased by 95% in ECIRS1 TG versus WT mice on NC. However, HF feeding decreased EC levels by 72% in WTHF mice compared with WT mice ($P < 0.01$). Similarly, ECIRS1 HF-fed mice also had 64% less EC than ECIRS1 TG mice (Fig. 6*A* and *B*). However, EC levels in the GT were significantly increased by 95% in ECIRS1 TG versus WT mice (Fig. 6*B*). IRS1

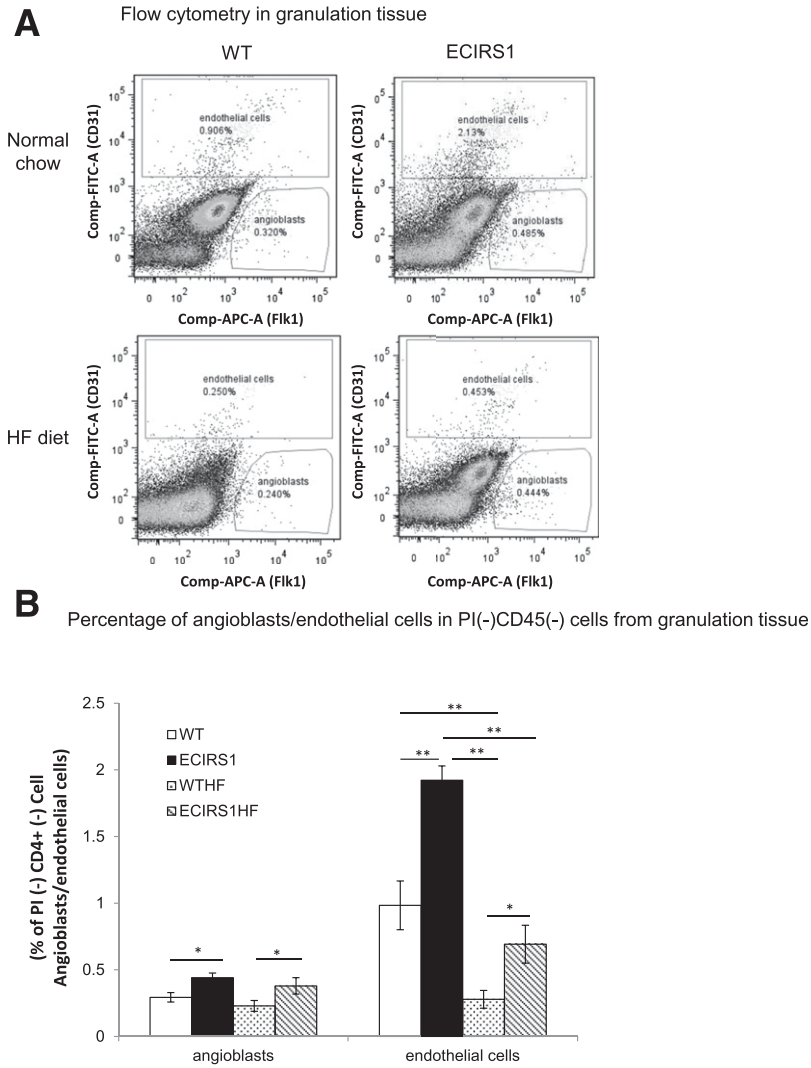

Figure 6—Characterization of angioblasts and ECs in GT by flow cytometry at 7 days postsurgery in WT, ECIRS1, WTHF, and ECIRS1HF mice. *A*: Angioblasts: $PI^-CD45^-Flk1^+CD31^-$; ECs: $PI^-CD45^-Flk1^{-/+}CD31^+$. *B*: Percentage of angioblasts and ECs in PI^-CD45^- cells. $^*P < 0.05$; $^{**}P < 0.01$. $n = 5$.

overexpression in the EC only partially restored its reduction induced by HF feeding and diabetes with elevation of ECs by 150% in ECIRS1 HF versus WTHF mice (Fig. 6*B*).

DNA synthesis of ECs and angioblasts was measured by BrdU incorporation in GT and BM. Figure 7*A* showed that proliferation of angioblasts in the GT was increased by 47% in ECIRS1 TG versus WT mice ($P < 0.05$), but no differences in BrdU incorporation were noted in these cells in the BM (Fig. 7*B*). To determine whether the elevation of angioblasts and ECs in the GT of ECIRS1 TG mice could also be due to uptake from circulation rather than proliferation in situ, the uptake of circulating Lin^- and GFP^+ cells, which were negative for PI, B220, CD4, CD8, Ter119, CD11b, and Ly6G cells and isolated from BM of GFP^+ mice, were infused into WT and ECIRS1 TG mice. Figure 7*C* and *D* showed that no increases of GFP^+ cells in the GT of ECIRS1 TG or WT mice were observed.

Analysis of Insulin's Signaling in Isolated Angioblasts and ECs From GT

To support the findings that insulin actions could be inhibited by HF diet and positively enhanced by IRS1 overexpression in ECs of ECIRS1 TG mice, IRS1 expressions and signal changes in pAkt were studied in angioblasts and ECs isolated from the GT. The results showed that IRS1 expression was increased specifically in the ECs of ECIRS1 TG mice by 291% ($P < 0.01$), but not in the angioblasts (Fig. 8*A* and *B*). IRS1 expression was associated with the expression of VE-cadherin since its promoter was used in the transgene to make ECIRS1 TG mice (Supplementary Fig. 1*A*). VE-cadherin expressions were only observed in ECs but not in angioblasts (Fig. 8*C*). The levels of pAkt stimulated by insulin (100 nmol/L) were similar in angioblasts from TG and WT mice (Fig. 8*D*) as assessed by FACS using antibodies to pAkt. Similarly, HF feeding did not affect pAkt levels in angioblasts from WT or ECIRS1TG

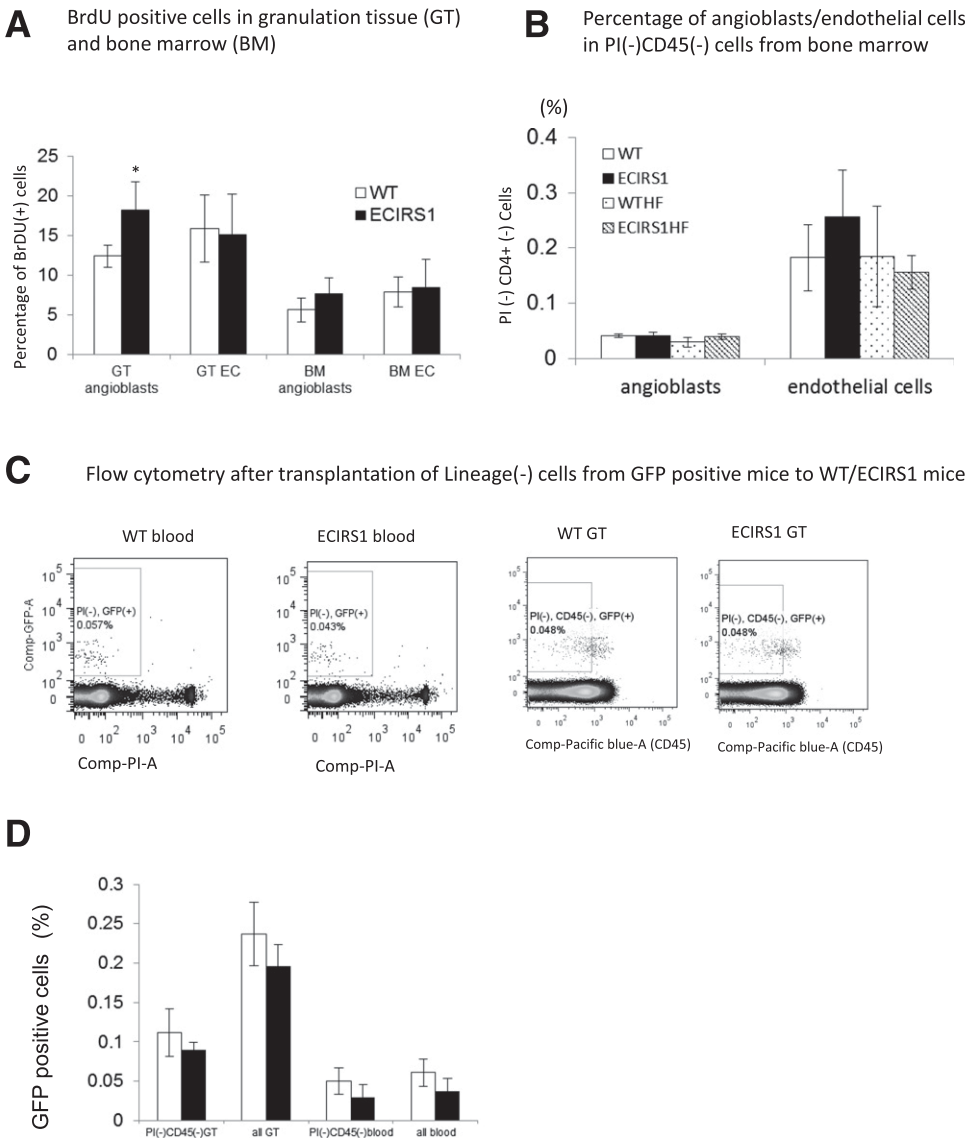

Figure 7—Analysis of angioblast and EC proliferation and uptake in GT 7 days after surgery in WT and ECIRS1 TG mice. *A*: BrdU$^+$ cells in BM (n = 7). *B*: Percentage of angioblasts and ECs in PI$^-$CD45$^-$ cells in BM. *C*: Flow cytometry analysis of uptake of lineage-negative cells in GT (n = 6). *D*: GFP$^+$ cells (%) in GT and blood 7 days after cell transplantation from GFP mice to WT and ECIRS1 TG mice. *P < 0.05.

mice. Unlike angioblasts, insulin-induced pAkt levels in ECs from GT were significantly higher, by 196%, in ECIRS1TG mice compared with WT mice (Fig. 8*E*). In contrast, insulin-induced pAkt levels only increased by 127% in ECs isolated from HF-fed ECIRS1HF compared with WTHF mice (Fig. 8*E*). Unlike the angioblasts, the levels of pAkt were significantly lower, by 50%, in the ECs of GT from ECIRS1 HF mice versus from WT mice on NC (Fig. 8*E*). Similarly, pAkt levels in the ECs from ECIRS1 HF were decreased by 64% versus ECIRS1 TG mice. Nevertheless, insulin-induced pAkt levels in ECs from ECIRS1 HF mice were still significantly higher than those from WTHF mice, by 107% (Fig. 8*E*). The levels of pAkt stimulated by VEGF (2.5 ng/mL) in angioblasts from GT were significantly higher in WT mice compared with WTHF mice (Fig. 8*F*).

DISCUSSION

This study demonstrated that enhancing insulin actions in the ECs can improve wound healing in nondiabetic, diabetic, and insulin-resistant states when insulin is present. Further, we have identified a novel defect in the differentiation of angioblast to EC with a parallel reduction of insulin-induced pAkt as a potential mechanism for the deficiency in angiogenesis in the GT induced by diabetes and insulin resistance.

Our study confirmed that diabetes, whether due to insulin deficiency or insulin resistance by HF diet, can impair both angiogenesis and the wound healing process (6,38,39). However, mechanisms causing the impaired wound healing process may be different when diabetes is due to insulin deficiency or obesity and insulin resistance. In the insulin deficiency model, enhancement of insulin

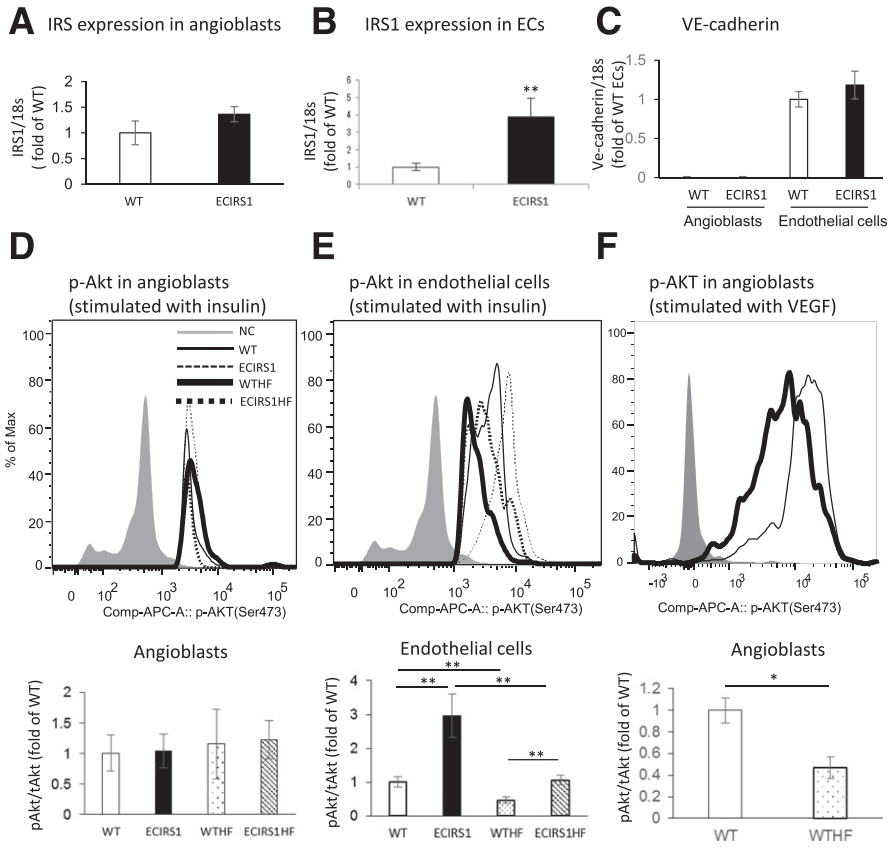

Figure 8—Expression and insulin/VEGF activation of signaling molecules in angioblasts and ECs in GT from WT, ECIRS1, WTHF, and ECIRS1HF mice. *A*: IRS1 mRNA expression in angioblasts. *B*: IRS1 mRNA expression in ECs of WT and ECIRS1 TG mice. *C*: VE-cadherin mRNA expression in angioblasts and ECs. Analysis for insulin-induced (100 nmol/L) Akt phosphorylation in angioblasts (*D*) and ECs (*E*). *F*: Analysis for VEGF-induced (2.5 ng/mL) Akt phosphorylation in angioblasts by using flow cytometry measuring the mean of the peak of fluorescent intensity. $^{*}P < 0.05$; $^{**}P < 0.01$. $n = 5$. tAkt, total Akt.

action in the ECs did not have any beneficial effects on wound healing, which supports the conclusion that the improvement in ECIRS1 TG mice was likely due to the enhancing of insulin's actions in the ECs of the GTs. Evaluation of the GT in ECIRS1 TG mice showed a sequential elevation of VEGF, FLK1, and VE-cadherin expressions after the initial injury compared with WT mice. These findings strongly supported the idea that improving insulin's actions in ECs enhanced VEGF expression and its signaling cascades to improve angiogenesis and wound healing. It is also possible that insulin may have perivascular effects due to its specific action on the ECs, such as the activation eNOS, to elevate NO and blood flow from the increases in angiogenesis to enrich the cells of the GT and improve wound healing (20,33,34,40). Further, increased blood flow to GT has been reported to improve the influx of inflammatory cells, which can enhance angiogenesis (21). Clearly, the elevated VEGF expression in the GT observed in ECIRS1 TG mice is likely due to the enhancement of insulin signaling through the IRS1/PI3K/Akt pathway, which has been shown to regulate VEGF expression in ECs (14,40,41).

The reduced VEGF expression in the GT from STZ-induced diabetic mice, which has been reported, is likely due to insulin deficiency (3,6,42). This conclusion is supported by the findings of the paradoxical increases of VEGF expression in GT from mice with HF-induced diabetes, which exhibited hyperinsulinemia rather than insulin deficiency. Hyperinsulinemia may induce VEGF not only in ECs but from fibroblasts and inflammatory cells (14,42). The paradoxical findings of VEGF expression in GT indicate that the impaired angiogenesis in wound healing may have different pathogenic mechanisms for insulin-resistant and deficiency-induced diabetes. This study provided the first direct comparative analysis of GT and wound healing between insulin-deficient and hyperinsulinemic and insulin-resistant models of diabetes. A previous report showed that VEGF expression in whole wound from HF-fed mice was similar to control diet, but higher than *ob/ob* diabetic mice (39).

Interestingly, HF-induced obesity clearly caused defects in GT formation and angiogenesis with decreased capillary density, even in the presence of hyperinsulinemia, and elevated VEGF levels, suggesting the possibility of resistance to insulin or VEGF actions in the GT of WTHF or ECIRS1HF mice. Analysis of GT cells indicated that enhancing EC's insulin action increased both angioblasts

and ECs. Interestingly, diabetes and insulin resistance inhibited only ECs and not angioblasts in the GT numbers. This provided the first identification that defect in capillary formation in GT induced by diabetes or insulin resistance is partly due to a selective inhibition in the differentiation of angioblasts to ECs. Further, the reduction of ECs could only be partially normalized by improving insulin's signaling in the ECs, even though VEGF levels were elevated in HF conditions. Our results also provide evidence that insulin can have actions on angioblasts, as shown by increasing DNA synthesis of angioblasts in the GT of ECIRS1 TG mice may not be inhibited by obesity or diabetes since angioblast numbers were not changed in these states. The effect of insulin to increase angioblasts and ECs in the GT was the result of elevating in situ cellular proliferation since there were no increases in the uptake from infused GFP-labeled angioblasts or ECs in WT or ECIRS1 TG mice. Signaling studies indicated that HF diet–induced selective inhibition of insulin induced pAkt in the ECs but not in the angioblasts, which is consistent with the finding that HF diet did not decrease the number of angioblasts but only the ECs. These findings confirmed the idea that diabetes and insulin resistance caused a selective defect in the differentiation of angioblasts to ECs. By using the VE-cadherin promotor, IRS1 overexpression is limited to ECs and not in angioblasts, which do not express VE-cadherin (43). This approach may not enhance angioblast differentiation to ECs, which appears to be abnormal also in diabetes. This study suggests that angioblasts are sensitive to insulin. Previously, Schatteman et al. (44) reported that circulating angioblasts responded initially to insulin at 6–12 μg/mL, but they become resistant after prolonged exposure, which the authors suggested is the reason that the hyperinsulinemia of type 2 diabetes could be causing poor angiogenesis in wound healing. However, the level of insulin used by Schatteman et al. (44), was ≈1 μmol/L, which is much higher than physiological levels (<10 nmol/L), which makes the finding difficult to interpret for in vivo studies.

These studies provide documentation that diabetes caused by insulin deficiency or diet-induced obesity can induce a selective abnormality in the differentiation of angioblasts to ECs in the GT, which is related to resistance of pAkt activation induced by insulin and possibly VEGF. Detailed studies to understand the mechanisms that are causing the inhibition of insulin or VEGF activation of pAkt in the GT in diabetes will need to be performed in the future. Further, we also observed that enhancing insulin action specifically in the ECs through the IRS1/PI3K/pAkt pathway could improve wound healing both in nondiabetic and obesity-induced diabetes, suggesting a new therapeutic target for wound healing.

Acknowledgments. The authors thank Scott Gordon at the Joslin Diabetes Center for the preparation of the manuscript.

Funding. S.K. is the recipient of a research fellowship (Hiroo Kaneda Scholarship, Sunstar Foundation, Japan). Support was also provided by the National Institute of Diabetes and Digestive and Kidney Diseases (NIDDK) Diabetes Research Center grant P30DK036836 and Grant-in-Aid for Scientific Research from the Japan Society for the Promotion of Science (26463128). This work was also supported by NIH/NIDDK grant R01 DK053105-13 to G.L.K.

Duality of Interest. No potential conflicts of interest relevant to this article were reported.

Author Contributions. S.K. performed most of the experiments and wrote the first draft of the manuscript. K.P., Y.M., M.K., Q.L., and H.Y. assisted in some studies and reviewed the manuscript. T.N.R. and A.W. provided advice on the analysis of the angioblasts and ECs from GT and BM. A.M. made the ECIRS1 TG mouse. L.L. and D.P.O. provided expertise on the wound healing model. G.L.K. conceived the project, designed the experiments, supervised all studies, and wrote the manuscript. G.L.K. is the guarantor of this work and, as such, had full access to all the data in the study and takes responsibility for the integrity of the data and the accuracy of the data analysis.

References

1. Boulton AJ, Vileikyte L, Ragnarson-Tennvall G, Apelqvist J. The global burden of diabetic foot disease. Lancet 2005;366:1719–1724

2. Brandner JM, Zacheja S, Houdek P, Moll I, Lobmann R. Expression of matrix metalloproteinases, cytokines, and connexins in diabetic and nondiabetic human keratinocytes before and after transplantation into an ex vivo wound-healing model. Diabetes Care 2008;31:114–120

3. Wetzler C, Kämpfer H, Stallmeyer B, Pfeilschifter J, Frank S. Large and sustained induction of chemokines during impaired wound healing in the genetically diabetic mouse: prolonged persistence of neutrophils and macrophages during the late phase of repair. J Invest Dermatol 2000;115:245–253

4. Lerman OZ, Galiano RD, Armour M, Levine JP, Gurtner GC. Cellular dysfunction in the diabetic fibroblast: impairment in migration, vascular endothelial growth factor production, and response to hypoxia. Am J Pathol 2003;162:303–312

5. Falanga V. Wound healing and its impairment in the diabetic foot. Lancet 2005;366:1736–1743

6. Brem H, Tomic-Canic M. Cellular and molecular basis of wound healing in diabetes. J Clin Invest 2007;117:1219–1222

7. Thangapazham RL, Darling TN, Meyerle J. Alteration of skin properties with autologous dermal fibroblasts. Int J Mol Sci 2014;15:8407–8427

8. Driskell RR, Lichtenberger BM, Hoste E, et al. Distinct fibroblast lineages determine dermal architecture in skin development and repair. Nature 2013;504:277–281

9. Thangarajah H, Yao D, Chang EI, et al. The molecular basis for impaired hypoxia-induced VEGF expression in diabetic tissues. Proc Natl Acad Sci U S A 2009;106:13505–13510

10. Brownlee M. Biochemistry and molecular cell biology of diabetic complications. Nature 2001;414:813–820

11. Wendt T, Harja E, Bucciarelli L, et al. RAGE modulates vascular inflammation and atherosclerosis in a murine model of type 2 diabetes. Atherosclerosis 2006;185:70–77

12. Koya D, King GL. Protein kinase C activation and the development of diabetic complications. Diabetes 1998;47:859–866

13. Geraldes P, King GL. Activation of protein kinase C isoforms and its impact on diabetic complications. Circ Res 2010;106:1319–1331

14. He Z, Opland DM, Way KJ, et al. Regulation of vascular endothelial growth factor expression and vascularization in the myocardium by insulin receptor and PI3K/Akt pathways in insulin resistance and ischemia. Arterioscler Thromb Vasc Biol 2006;26:787–793

15. Miele C, Rochford JJ, Filippa N, Giorgetti-Peraldi S, Van Obberghen E. Insulin and insulin-like growth factor-I induce vascular endothelial growth factor mRNA expression via different signaling pathways. J Biol Chem 2000;275:21695–21702

16. Apikoglu-Rabus S, Izzettin FV, Turan P, Ercan F. Effect of topical insulin on cutaneous wound healing in rats with or without acute diabetes. Clin Exp Dermatol 2010;35:180–185
17. Madibally SV, Solomon V, Mitchell RN, Van De Water L, Yarmush ML, Toner M. Influence of insulin therapy on burn wound healing in rats. J Surg Res 2003; 109:92–100
18. Wilson JM, Baines R, Babu ED, Kelley CJ. A role for topical insulin in the management problematic surgical wounds. Ann R Coll Surg Engl 2008;90:160
19. Rezvani O, Shabbak E, Aslani A, Bidar R, Jafari M, Safarnezhad S. A randomized, double-blind, placebo-controlled trial to determine the effects of topical insulin on wound healing. Ostomy Wound Manage 2009;55:22–28
20. Lima MH, Caricilli AM, de Abreu LL, et al. Topical insulin accelerates wound healing in diabetes by enhancing the AKT and ERK pathways: a double-blind placebo-controlled clinical trial. PLoS One 2012;7:e36974
21. Gurtner GC, Werner S, Barrandon Y, Longaker MT. Wound repair and regeneration. Nature 2008;453:314–321
22. Somanath PR, Chen J, Byzova TV. Akt1 is necessary for the vascular maturation and angiogenesis during cutaneous wound healing. Angiogenesis 2008;11:277–288
23. Hinz B. Formation and function of the myofibroblast during tissue repair. J Invest Dermatol 2007;127:526–537
24. Somanath PR, Kandel ES, Hay N, Byzova TV. Akt1 signaling regulates integrin activation, matrix recognition, and fibronectin assembly. J Biol Chem 2007; 282:22964–22976
25. Werner S, Krieg T, Smola H. Keratinocyte-fibroblast interactions in wound healing. J Invest Dermatol 2007;127:998–1008
26. Goren I, Müller E, Schiefelbein D, et al. Akt1 controls insulin-driven VEGF biosynthesis from keratinocytes: implications for normal and diabetes-impaired skin repair in mice. J Invest Dermatol 2009;129:752–764
27. Nakai K, Yoneda K, Moriue T, Igarashi J, Kosaka H, Kubota Y. HB-EGF-induced VEGF production and eNOS activation depend on both PI3 kinase and MAP kinase in HaCaT cells. J Dermatol Sci 2009;55:170–178
28. Park K, Mima A, Li Q, et al. Insulin's novel mechanis, to decrease atherosclerosis by unducing ETBR expression. JCI Insight 2016;1:e86574
29. Rask-Madsen C, Li Q, Freund B, et al. Loss of insulin signaling in vascular endothelial cells accelerates atherosclerosis in apolipoprotein E null mice. Cell Metab 2010;11:379–389
30. Pietramaggiori G, Scherer SS, Mathews JC, et al. Quiescent platelets stimulate angiogenesis and diabetic wound repair. J Surg Res 2010;160:169–177
31. Pietramaggiori G, Kaipainen A, Ho D, et al. Trehalose lyophilized platelets for wound healing. Wound Repair Regen 2007;15:213–220
32. Succar J, Douaiher J, Lancerotto L, et al. The role of mouse mast cell proteases in the proliferative phase of wound healing in microdeformational wound therapy. Plast Reconstr Surg 2014;134:459–467
33. Park K, Li Q, Rask-Madsen C, et al. Serine phosphorylation sites on IRS2 activated by angiotensin II and protein kinase C to induce selective insulin resistance in endothelial cells. Mol Cell Biol 2013;33:3227–3241
34. Li Q, Park K, Li C, et al. Induction of vascular insulin resistance and endothelin-1 expression and acceleration of atherosclerosis by the overexpression of protein kinase C-β isoform in the endothelium. Circ Res 2013;113:418–427
35. Song G, Nguyen DT, Pietramaggiori G, et al. Use of the parabiotic model in studies of cutaneous wound healing to define the participation of circulating cells. Wound Repair Regen 2010;18:426–432
36. Rao TN, Marks-Bluth J, Sullivan J, et al. High-level Gpr56 expression is dispensable for the maintenance and function of hematopoietic stem and progenitor cells in mice. Stem Cell Res (Amst) 2015;14:307–322
37. Seth AK, De la Garza M, Fang RC, Hong SJ, Galiano RD. Excisional wound healing is delayed in a murine model of chronic kidney disease. PLoS One 2013; 8:e59979
38. Moura J, Børsheim E, Carvalho E. The role of microRNAs in diabetic complications-special emphasis on wound healing. Genes (Basel) 2014;5:926–956
39. Seitz O, Schurmann C, Hermes N, et al. Wound healing in mice with high-fat diet- or ob gene-induced diabetes-obesity syndromes: a comparative study. Exp Diabetes Res 2010;2010:476969
40. Maeno Y, Li Q, Park K, et al. Inhibition of insulin signaling in endothelial cells by protein kinase C-induced phosphorylation of p85 subunit of phosphatidylinositol 3-kinase (PI3K). J Biol Chem 2012;287:4518–4530
41. Taylor SM, Nevis KR, Park HL, et al. Angiogenic factor signaling regulates centrosome duplication in endothelial cells of developing blood vessels. Blood 2010;116:3108–3117
42. Khamaisi M, Katagiri S, Keenan H, et al. PKCδ inhibition normalizes the wound-healing capacity of diabetic human fibroblasts. J Clin Invest 2016;126:837–853
43. Giannotta M, Trani M, Dejana E. VE-cadherin and endothelial adherens junctions: active guardians of vascular integrity. Dev Cell 2013;26:441–454
44. Schatteman GC, Hanlon HD, Jiao C, Dodds SG, Christy BA. Blood-derived angioblasts accelerate blood-flow restoration in diabetic mice. J Clin Invest 2000; 106:571–578